Optics Letters

Object extraction from underwater images through logical stochastic resonance

Bing Zheng, Nan Wang,* Haiyong Zheng, Zhibin Yu, and Jinpeng Wang

Ocean University of China, Qingdao 266100, China
**Corresponding author: wangnanseu@163.com*

Received 29 July 2016; revised 19 September 2016; accepted 22 September 2016; posted 23 September 2016 (Doc. ID 272605); published 25 October 2016

Logical stochastic resonance (LSR), the phenomenon in which the interplay of noise and nonlinearity can raise the accurate probability of response to feeble input signals, is studied in this Lettter to extract objects from highly degraded underwater images. Images captured under water, especially in the turbid areas, always suffer from interference through heavy noise caused by the suspended particles. Inherent noise and nonlinearity cause difficulty in processing these images through conventional image processing methods. However, LSR can optimally address such issues. A heavily degraded image is first extended to a 1D form in the direction determined by the illumination condition, and then normalized to be placed in the LSR system as an input signal. Additional Gaussian noise is added to the system as the auxiliary power to help separate the object and the background. Results in the natural offshore area demonstrate the effect of LSR on image processing, and the proposed method creates an interesting direction in the processing of heavily degraded images.

OCIS codes: (030.4280) Noise in imaging systems; (100.0100) Image processing.

http://dx.doi.org/10.1364/OL.41.004967

In recent years, underwater vision has received increasing attention because of abundant marine resources and the high research value of oceans. However, the fundamental limits imposed by the underwater environment, such as absorption and scattering of light by particles in the water, constrain the quality of underwater imaging [1]. Moreover, underwater images show large temporal and spatial variations [2]. These problems cause difficulty in building an accurate physical model [3] and in processing underwater images through the conventional image processing methods.

Two main inherent characteristics of turbid media imaging are nonlinearity and heavy noise. However, the noise is not always detrimental. Stochastic resonance (SR) [4] is the typical theory of noise being useful. With the interplay of nonlinearity and noise, SR is particularly helpful in processing a feeble signal which is overwhelmed by heavy noise [5,6]. Furthermore, recently in the field of image processing, the application of SR in denoising, image enhancement, and edge detection has been reported [7–11]. Although the aforementioned studies have obtained a good effect, the SR concept is only used as a supplement to the conventional image processing methods, such as histogram analysis and Fourier transformation.

On the basis of SR, the concept of logical stochastic resonance (LSR), which extended the SR concept to *s* logical system [12,13], is proposed. The typical phenomenon of LSR is that the response of a bistable system to two feeble inputs can obtain a logical output with accuracy controlled by noise intensity, and the logical function can be easily tuned by modulating the system parameters. As we know, the ultimate aim of object detection is to detect and extract an object from the background, which is a logical judgment procedure. Thus, using LSR to process heavily degraded images captured under turbid media may be helpful.

In this Letter, as we only aim at object detection and extraction from the heavily noisy background, only two logical states (0 and 1) are needed. We consider logic 0 as the background and logic 1 as the object. Given only two states, we choose the popular quartic-bistable dynamical system as the base nonlinear system, which is governed by (1):

$$U(x) = \frac{b}{4}x^4 - \frac{a}{2}x^2 - rx, \tag{1}$$

where $U(x)$ represents the bistable potential system. a and b are the coefficients of linear and nonlinear terms, respectively. When the bias r is zero, the system (1) has two stable states at $x_\pm = \pm\sqrt{a/b}$ and a potential barrier with $\Delta V = a^2/4b$ at 0. r has the effect of asymmetrizing the two potential wells to achieve different output logic. Figure 1 shows the potential well of system (1) with a different bias r. We can observe that by changing the bias r, the bistable states become asymmetric, and the potential barrier is changed. When the potential well is symmetric, and the barrier is not high, particles jump arbitrarily between the two wells under the effect of additional power offered by the noise. However, if the potential well is not symmetric, according to Langevin dynamics, particles in such a system have a greater likelihood of jumping into and staying in the low-potential well. Thus, by tuning the potential well, we can detect a feeble signal by helping the corresponding

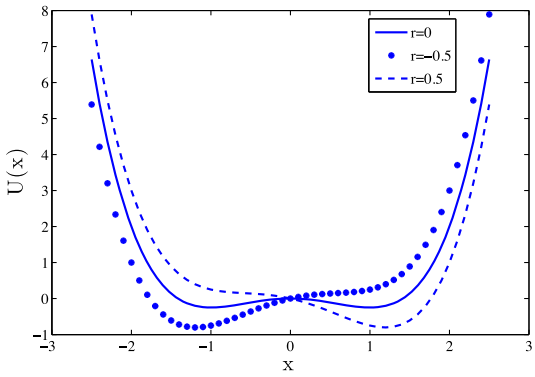

Fig. 1. Potential well of system (1) to the different bias r.

pixels jump to the right potential well and manage the output logic according to specific applications at the same time.

When the system is driven by a feeble signal together with heavy noise, the Langevin function of (1) can be written as

$$\dot{x} = \dot{U}(x) + I(t) + D\eta(t), \tag{2}$$

with the nonlinear system $U(x)$ given by Eq. (1); $\eta(t)$ denotes Gaussian white noise with zero mean and delta correlation, and D is the noise intensity. $I(t)$ is the low-amplitude input signal. $t(t \geq 0)$ is the index of the sampling. When $I(t)$ is a time-varying signal; t can represent the sampling time. When I represents an image signal, t can be considered as the pixel coordinates.

The framework of the LSR-based object extraction of a highly degraded image is shown in Fig. 2. The pipeline has two main streams. One is the input-output stream. We set the heavily degraded image as the input signal. Additional noise, the density of which is decided by the inherent noise of the image, is added at the same time to the nonlinear system. The additional noise is used to counter the inherent noise. The output end of the system is the labeled result, which can directly indicate whether a pixel belongs to the object or the background. The other stream of the pipeline takes the role of parameter modulating. To make the system adaptive, the major feature of the given image is calculated and used as the adaption algorithm input. In this Letter, noise intensity and illumination direction are considered to decide the system parameters: a, b, and r.

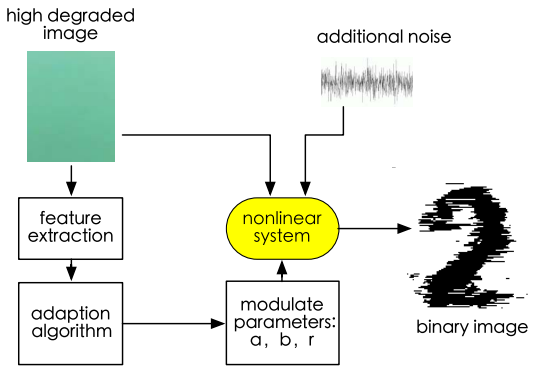

Fig. 2. Main framework of the LSR-based object extraction of a highly degraded image.

The general format of the input in traditional LSR is 1D. However, an image is universally 2D. Thus, before using LSR to deal with the image information, we have to reduce the dimension first. Imaging through turbid water suffers interference not only through the noise caused by suspended particles, but also through non-uniformed illumination. Because of the highly nonuniformed illumination, the overall image intensity changes in the direction of the illumination. Based on this observation, the image can be extended to 1D in the direction perpendicular to the illumination direction. Moreover, the underwater imaging can be classified as natural and artificial lighting. Regardless of the type of illumination, the illumination direction can be estimated by an illumination direction estimation algorithm. In this Letter, the main procedure of illumination estimation involves finding the point with the highest intensity, and then calculating the changing direction. Once the illumination direction is obtained, the image can be processed.

When the zenith angle is larger than 45°, for example, during crepuscular time, the illumination is dominated by horizontal changes. We can extend the image to 1D through the column and consider the row information as auxiliary at the same time. When the zenith angle is considerably small, such as at noon, the image is dominated by the vertical illumination changes, and we can extend the image mainly by array and, at the same time, consider the column information. When the illumination is multidirectional, such as using artificial lighting, we can also extend the image in the perpendicular direction combined with anisotropic filter, which is used to smooth the captured image to estimate the illumination direction more accurately. Then, the intensity of every pixel has to be normalized to [0, 1].

In our experiments, we mainly use the image captured in Jiaozhou Bay in northeast China. The camera used in our experiment is a 411,000-pixel CCD sensor (UWC-300, Outland Technology). The camera and the illumination system are installed on a tow sled. The artificial illumination is powered with a 150 W halogen bulb. The underwater visibility is an important characteristic of water quality and, at the same time, a crucial parameter which will determine the final quality of underwater imaging. The classical method of measuring water quality is by the Secchi disk method [14]. In our experiment, the Secchi depth is measured as 1.7 m. The Secchi depth is a very intuitive instruction, but not very precise. Thus, we also use the AC-S meter(WET-LABS) to measure water attenuation and absorption coefficients. The corresponding measured coefficients are 3.9 m^{-1} and 0.95 m^{-1}, respectively. According to statistics, the typical attenuation coefficients for deep ocean water, coastal water, and bay water are 0.05 m^{-1}, 0.2 m^{-1}, and 0.33 m^{-1}, respectively, and the transparent quality decreases successively. Therefore, the experimental data on water quality show that the test water area is more turbid than the areas considered in most studies on underwater image processing.

When the underwater visibility is preferable, the major problems in underwater images are low contrast and color distortion. Correspondingly, the color correction and contrast enhancement algorithm, such as white balance and histogram equalization, can be used to produce a visually pleasing image. However, when the attenuation coefficient of the water area is large, the underwater images not only suffer from the above problems, but also from the high noise, which makes the image almost unacceptable and difficult to deal with.

A group of heavily degraded images captured in our experiments and the corresponding results processed by two different methods, which are state-of-the-art algorithms, are presented in Fig. 3. The images in the first row of Fig. 3 are the original images, which are the imaging of the calibration board from different conditions. Numbers 1, 2, 3, and 4 and some calibration tails are printed on the calibration board. The entire board is approximately 60 cm × 40 cm, and each number is about 10 cm × 5 cm. The distance from the camera to the object is 1, 1, and 1.2 m. The illumination type is natural light in Fig. 3(a) and artificial light in Figs. 3(b) and 3(c), respectively. The raw pictures clearly show a blue–green tone that coincides with the scattering feature of seawater. Since the water visibility is poor, the pictures have a low quality characterized by a high-intensity noise and a low contrast. Such highly degraded images are the object of this Letter. Our goal is to correctly detect the shape of the characters on the calibration board without any pre-processing procedure.

As indicated in Fig. 3, popular processing methods may slightly enhance the visibility, but the enhancement is feeble. Detecting clear information from these images by traditional image segmentation method is still difficult, since the pre-processing images also have poor quality.

In the three raw pictures shown in Fig. 3, Fig. 3(b) is relatively simple to process than the other images. Thus, we use this image to show the capacity of LSR in underwater image processing first. The focus of the illumination in Fig. 3(b) is almost at the center of the image and, under the effect of this, numbers 1 and 3 are much clearer than numbers 2 and 4. In the conventional image processing method, the morphological method is always used to subtract the effect of a nonuniformed background. However, in Fig. 3(b), the background and the object are already blended together because of the high-intensity noise. Thus, filtering the effect of the nonuniformed light under the influence of heavy noise with the morphological method is very difficult. However, we can resort to LSR to solve this problem effectively. The aforementioned bistable potential well is used as the base system, and the parameters are set to be $a = 1.25$, $b = 0.5$, $r = 0.4$. Gaussian white noise is also additionally. Figure 4 is the result obtained by the proposed method

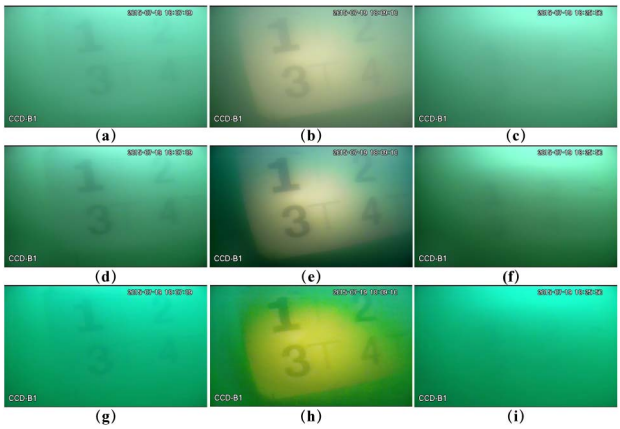

Fig. 3. Heavily degraded underwater images enhancement test by state-of-the-art algorithm. (a)–(c) Raw image captured in Jiaozhou Bay in 3 m depth. (d)–(f) Results of a dark channel algorithm [15]. (g)–(i) Results of the Tarel algorithm [16].

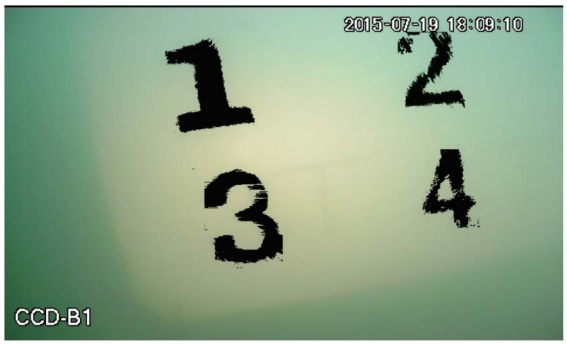

Fig. 4. Image of Fig. 3(b) processed by our method.

when additional noise intensity is 0.4. As this figure shows, our approach can detect the object perfectly.

In Fig. 3(a), the numbers on the object plate are fuzzier than those with additional artificial light. We can only recognize that there are several numbers in the pictures. However, the contour detail is very vague, especially in numbers 2 and 4. Furthermore, the picture is also affected by the nonuniform illumination; even the illumination is not very clear to human vision. The image is lighter at the right-top, and much darker at the bottom. If we use the classical threshold method to process this image, the illumination effect will be dominated. To narrow down the computing range and obtain a convenient explanation, we first manually sketched the regions that seem to have a number, such as the red boxes in Fig. 5(a). The pixel-wise intensity color map and corresponding LSR processed result of each ROI region are shown in Figs. 5(b)–5(i). Carefully observing the color map, we find that the object information is almost drowned by the noise. The highly degraded image is used as the input of the potential well, which is supported by the additional noise, and the nonlinear system

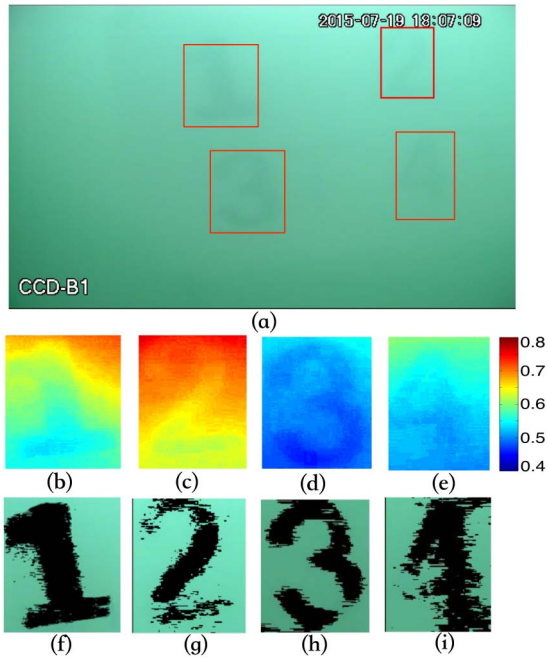

Fig. 5. (a) Sketched ROI, (b)–(e) a density color map of each number, and (f)–(i) the labeled result of each number.

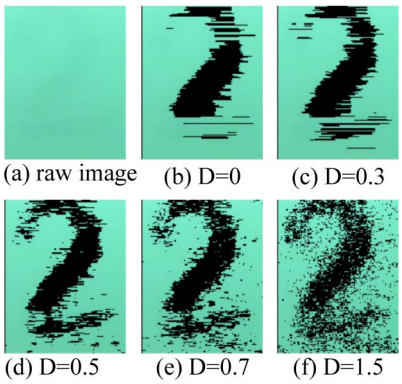

Fig. 6. (a) Raw image and (b)–(f) labeled result with different noise intensity.

can help to separate the feeble signal from the high-intensity noise. Thus, the correctly labeled result is presented in the output end.

Furthermore, to testify the effect of LSR, we change the noise intensity to observe the result. Without a loss of generality, number 2 is taken as an example. When the additional noise is zero, we do not add any noise, but only place the cropped image as the input signal to the potential well. The output image cannot show the number 2 figure correctly [Fig. 6(b)]. However, as the noise intensity is raised, a much clearer shape of the number shows up. For example, when the noise intensity is about 0.5, the number can be separated from the background easily, as shown in Fig. 6(d). If we continually raise the noise intensity, the noise on the output image begins to increase. When the noise intensity is more than 1, the useful information is drowned by the noise in the output end again, as shown in Fig. 6(f). Figure 7 indicates that the correct probability changes nonmonotonically as the noise intensity increases. The probability first increases to almost 1 and then decreases versus noise intensity, which is the typical character of SR.

We have shown the ability of the LSR-based method in object detection from heavily degraded underwater images. At last, we will test the limit of the proposed method by Fig. 3(c). As we see, Fig. 3(c) is too blurry, and useful information is hardly visible in this picture. However, if we process this picture with our algorithm, we obtain the result as Fig. 8. The picture clearly contains four numbers, and we can easily recognize 1, 2, and 3 in this processed image. Number 4 is the most unclear number, because the right bottom corner of the image is overwhelmed by noise. Although the shapes of the numbers are not

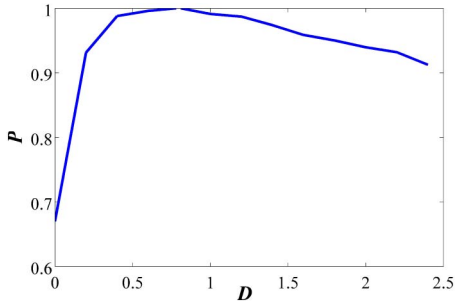

Fig. 7. Correct probability curve of the extraction result versus the noise intensity.

Fig. 8. Processed result of Fig. 3(c) by our method.

very clear, obviously, the signal-to-noise (SNR) ratio increases significantly after LSR processing.

In summary, we introduce the concept of LSR to deal with extremely noisy images captured under water. An image is extended to 1D signal in directions perpendicularly to the light direction. Experimental results show that the proposed method can help to raise the SNR ratio and effectively extract the number shape from the background. However, this new LSR-based method also presents certain problems, foremost of which is that it can only label the image through logical conditions. Furthermore, the LSR concept cannot solve the problem when the object is already completely drowned by noise. Despite these limitations, the LSR-based method proposed in this Letter presents a new direction to process highly degraded images captured under water.

Funding. China Postdoctoral Science Foundation (2016M590658); National Natural Science Foundation of China (NSFC) (61301240).

REFERENCES

1. J. S. Jaffe, IEEE J. Ocean. Eng. **40**, 683 (2015).
2. S. Raimondo and C. Silvia, EURASIP J. Adv. Sig. Process. **1**, 1 (2010).
3. G. Wang, B. Zheng, and F. F. Sun, Opt. Lett. **36**, 2384 (2011).
4. R. Benzi, A. Sutera, and A. Vulpiani, J. Phys. A **14**, L453 (1981).
5. A. A. Saha and G. V. Anand, Signal Process. **86**, 3466 (2006).
6. R. P. Morse, S. D. Holmes, and B. Shulgin, in *Conference on Noise and Fluctuations in Biological, Biophysical, and Biomedical Systems*, Florence, Italy, 2007.
7. C. Ryu, S. G. Kong, and H. Kim, Pattern Recogn. Lett. **32**, 107 (2011).
8. Q. Ye, H. Huang, and X. He, in *Proceedings. 2003 International Conference on Image Processing* (2003), Vol. **1**, p. 894.
9. A. Histace and D. Rousseau, Electron. Lett. **42**, 393 (2006).
10. S. Janpaiboon and S. Mitaim, "Adaptive stochastic resonance in color object segmentation," in *International Joint Conference on Neural Networks*, July, 2006, pp. 2508–2515.
11. R. K. Jha and R. Chouhan, Signal Image Video Process. **8**, 339 (2014).
12. K. Murali, I. Rajamohamed, S. Sinha, W. L. Ditto, and A. R. Bulsara, Appl. Phys. Lett. **95**, 194102 (2009).
13. K. Murali, S. Sinha, W. L. Ditto, and A. R. Bulsara, Phys. Rev. Lett. **102**, 194102 (2009).
14. J. Graham, Limnol. Oceanogr. **11**, 184 (1966).
15. K. He, J. Sun, and X. Tang, IEEE Trans. Pattern Anal. Mach. Intell. **33**, 2341 (2011).
16. J. P. Tarel and N. Hautiere, in *IEEE 12th International Conference on Computer Vision* (IEEE, 2009), pp. 2201–2208.